HOKKAIDO UNIVERSITY

| | |
|---|---|
| Title | Murine intestinal organoids resemble intestinal epithelium in their microRNA profiles |
| Author(s) | Ohsaka, Fumina; Sonoyama, Kei |
| Citation | Bioscience biotechnology and biochemistry, 82(9), 1560-1567<br>https://doi.org/10.1080/09168451.2018.1469397 |
| Issue Date | 2018-05-08 |
| Doc URL | http://hdl.handle.net/2115/73876 |
| Rights | This is an Accepted Manuscript of an article published by Taylor & Francis in Bioscience biotechnology and biochemistry on 08 May 2018, available online: http://www.tandfonline.com/10.1080/09168451.2018.1469397. |
| Type | article (author version) |
| Additional Information | There are other files related to this item in HUSCAP. Check the above URL. |
| File Information | Ohsaka2017BBB_R2 -fig.pdf |

Instructions for use

Hokkaido University Collection of Scholarly and Academic Papers : HUSCAP

# Murine intestinal organoids resemble intestinal epithelium in their microRNA profiles

Fumina Ohsaka [a] and Kei Sonoyama [b, *]

[a] Graduate School of Life Science, Hokkaido University, Sapporo, Hokkaido 060-8589, Japan

[b] Research Faculty of Agriculture, Hokkaido University, Sapporo, Hokkaido 060-8589, Japan

Running head: MicroRNAs in intestinal epithelial cells and organoids

* Corresponding author: Kei Sonoyama

Laboratory of Food Biochemistry, Division of Fundamental AgriScience Research, Research Faculty of Agriculture, Hokkaido University

Kita-9 Nishi-9, Kita-ku, Sapporo, Hokkaido 060-8589, Japan

Tel & Fax: +81-11-706-2496; E-mail: ksnym@chem.agr.hokudai.ac.jp

**Abstract**

Intestinal organoids were established as an *ex vivo* model of the intestinal epithelium. We investigated whether organoids resemble the intestinal epithelium in their microRNA (miRNA) profiles. Total RNA samples were obtained from crypt and villus fractions in murine intestine and from cultured organoids. Microarray analysis showed that organoids largely resembled intestinal epithelial cells in their miRNA profiles. *In silico* prediction followed by qRT-PCR suggested that six genes are regulated by corresponding miRNAs along the crypt-villus axis, suggesting miRNA regulation of epithelial cell renewal in the intestine. However, such expression patterns of miRNAs and their target mRNAs were not reproduced during organoids maturation. This might be due to lack of luminal factors and endocrine, nervous, and immune systems in organoids and different cell populations between *in vivo* epithelium and organoids. Nevertheless, we propose that intestinal organoids provide a useful *in vitro* model to investigate miRNA expression in intestinal epithelial cells.

**Keywords:** microRNA; intestinal epithelium; intestinal organoid; microarray

The epithelium of the small intestine is a self-renewing system undergoing continuous replacement from stem cells throughout the lifespan of an animal [1]. Morphologically, the epithelium consists of a single-cell layer that is organized into tubular invaginations called crypts and finger-like protrusions known as villi. The entire sequence of cell renewal, i.e., cell proliferation, cell differentiation, and cell death, is coupled to cell migration along the crypt-villus axis. Although the intestinal epithelium has been difficult to model in culture, the establishment of a system for culturing primary stem cell-derived intestinal organoids has overcome this difficulty [2-4]. Small intestinal organoids consist of a polarized epithelium that is patterned into villus-like regions containing differentiated enterocytes, goblet cells, and enteroendocrine cells; and crypt-like proliferative zones containing stem cells, transit-amplifying cells, and Paneth cells [2]. Thus, intestinal organoids recapitulate critical *in vivo* characteristics, such as the cellular composition and self-renewal kinetics of the intestinal epithelium [2].

MicroRNAs (miRNAs), a class of small noncoding RNA species, regulate gene expression by binding to partially complementary target sites in the 3'untranslated regions of mRNAs and then trigger either mRNA degradation or translational repression [5, 6]. miRNAs are involved in numerous biological process including cell proliferation, cell differentiation, and cell death [7]. In the intestine, a complete compendium of miRNAs, obtained by ultra-high throughput sequencing, has been reported [8]. In addition, miRNA expression profiles reportedly become altered during cell differentiation in the enterocyte-like cell line Caco-2-BBE [9]. Also, miRNA expression profiles are different between crypt and villus epithelial cells in murine small intestines [10]. Thus, it is possible that miRNAs are involved in the cell renewal process along the crypt-villus axis in the intestine, and intestinal organoids may offer a promising model to investigate the role of miRNAs. However, it has yet to be determined whether intestinal organoids recapitulate miRNA expression profiles in intestinal epithelial cells *in vivo*. The present study aimed to compare the miRNA profiles between murine intestinal epithelial cells and organoids in terms of changes in the crypt-villus axis and maturation process of organoids.

## Materials and methods

*Animal care.* Male C57BL/6J mice (age 5 weeks) were purchased from Japan SLC (Shizuoka, Japan) and housed in standard plastic cages in a temperature-controlled (23 ± 2°C) room under a 12-h light/12-h dark cycle and were allowed free access to tap water and standard laboratory rodent feed (Oriental Yeast, Tokyo, Japan). All study protocols were approved by the Animal Use Committee of Hokkaido University (approval no. 14-0028). Animals were maintained in accordance with the Hokkaido University guidelines for the care and use of laboratory animals.

*Isolation of intestinal villi and crypts and culture of organoids.* Mice were euthanized by cervical dislocation under sevoflurane anesthesia. A laparotomy was made, and the entire length of the small intestine was excised. The luminal contents were thoroughly washed out with ice-cold PBS, and the small intestine was opened longitudinally. The tissue was cut into approximately 5-mm pieces and further washed with ice-cold PBS. The tissue pieces were incubated in 2 mM EDTA/PBS for 60 min at 4°C followed by straining through gauze. The filtrates were centrifuged at 200 × *g* for 3 min, and the resultant precipitate was regarded as the villus fraction. The tissue pieces retained by the gauze were resuspended in 2 mM EDTA/PBS. After vigorous shaking and sedimentation, the supernatant was passed through a 70-μm cell strainer (BD Biosciences, San Jose, CA), followed by centrifugation at 200 × *g* for 3 min. The resultant precipitate was regarded as the crypt fraction. The villus and crypt fractions were viewed under a light microscope, snap-frozen in liquid nitrogen, and stored at –80°C for RNA isolation as described below. For intestinal organoids, the isolated crypts were cultured as previously described [11]. Organoids cultured for 1 day and 5 days were subjected to RNA isolation as described below.

*Isolation of RNA and quantitative real-time PCR (qRT-PCR) analysis.* Total RNA including small RNA was isolated from intestinal villus/crypt fractions and organoids using an miRNeasy Mini kit (Qiagen, Tokyo, Japan) according to the manufacturer's instructions. For

mRNA and miRNA analyses, first-strand cDNA was synthesized using ReverTra Ace qPCR RT Master Mix (Toyobo, Osaka, Japan) and miScript II RT kit (Qiagen, Tokyo, Japan), respectively, according to the manufacturers' instructions. For miRNA, synthetic *Caenorhabditis elegans* miRNA (Syn-cel-miR-39-3p, 0.25 fmol, Qiagen, Tokyo, Japan) was spiked in. qRT-PCR was performed using a Thermal Cycler Dice Real-Time System (Takara, Shiga, Japan). For mRNA, the qRT-PCR reaction was performed in a 12.5-μL reaction solution containing 6.25 μL of GeneAce SYBR qPCR Mix α No ROX (Nippongene, Toyama, Japan), 0.5 μL of 5 μM gene-specific primers (Supplementary Table 1), and 1 μL of first-strand cDNA sample. For miRNA, the qRT-PCR reaction was performed in a 12.5-μL reaction solution containing 6.25 μL of miScript SYBR Green PCR Master Mix (Qiagen, Tokyo, Japan), 1.25 μL of 10× miScript universal primer (Qiagen, Tokyo, Japan), 1.25 μL of 5 μM gene-specific primer (Supplementary Table 1), and 1 μL of first-strand cDNA sample. The qRT-PCR conditions were as follows: 95°C for 10 min, followed by 45 cycles at 95°C for 30 s and 60°C for 60 s, with dissociation at 95°C for 15 s, 60°C for 30 s, 95°C 15 s. The fluorescent products were detected at the last step of each cycle. The relative expression levels of mRNA and miRNA were normalized to that of β-actin and cel-miR-39-3p, respectively.

*miRNA microarray analysis.* Pooled samples in each group, the villus fraction (n=6), crypt fraction (n=6), organoids on day 1 (n=4), and organoids on day 5 (n=4), were subjected to miRNA expression profiling. Microarray analysis including labeling, hybridization, scanning, and data processing was performed by Toray Industries, Inc. using 3D-Gene mouse miRNA oligo chips ver. 21 that contains 1,900 antisense probe spots (Toray Industries, Tokyo, Japan). Using the background-subtracted signal intensity of all miRNAs in each microarray, the expression level of each miRNA was globally normalized such that the median of all miRNAs for each sample was 25. Microarray data is deposited as a MIAME compliant study in NCBI's Gene Expression Omnibus [12] and are accessible through GEO Series accession number GSE99237 (http://www.ncbi.nlm.nih.gov/geo/query/acc.cgi?acc=GSE99237). The heatmap image for differentially expressed miRNAs was processed using the Cluster 3.0 software

(http://bonsai.hgc.jp/~mdehoon/software/cluster/software.htm), and the results were visualized with the JAVA TreeView program (http://jtreeview.sourceforge.net/).

*In silico analyses.* For the prediction of miRNA targets, four web-based tools, Miranda (http://www.microrna.org/), miRDB (http://mirdb.org/), PicTar (http://pictar.mdc-berlin.de), and TargetScan (http://www.targetscan.org/), were used. The predicted genes were further narrowed down by their gene ontology (GO) classifications by the Mouse Genome Informatics resource (http://www.informatics.jax.org/).

*Statistical analyses.* Group differences were assessed by the Mann-Whitney *U* test. Correlations between miRNA profiles in the villus/crypt fractions and organoids were evaluated using Pearson's correlation coefficient (*r*). Data were analyzed using GraphPad Prism for Macintosh (version 6, GraphPad Software, San Diego, CA). *P* values $<0.05$ were considered to indicate statistical significance.

## Results

*Murine intestinal organoids resemble intestinal epithelium in their miRNA profiles.*

Light microscopic observation of crypt and villus fractions prepared from murine small intestine showed a typical morphological appearance of intestinal crypt and villus, respectively (Supplementary Fig. 1A and 1B, respectively). We then examined the mRNA levels of *Fabp2* and *Lgr5*, markers of differentiated enterocytes located on the villus [13] and of stem cells located on the crypt base [2], respectively. qRT-PCR showed that the *Fabp2* mRNA levels were significantly higher in the villus than in the crypt fraction (Supplementary Fig. 1C), and that *Lgr5* mRNA levels were significantly higher in the crypt than in the villus fraction (Supplementary Fig. 1D). These data suggest that crypts and villi were enriched separately in each fraction. In addition, we successfully cultured murine intestinal organoids (Supplementary Fig. 1E and 1F). On day 5 of culture, we observed the typical structure of mature intestinal organoids, consisting of a central cyst structure and surrounding crypt-like budding structures.

143 qRT-PCR showed that the mRNA levels of *Apoa1, Muc2*, and *Pyy*, differentiated enterocyte,
144 goblet cell, and enteroendocrine markers, respectively [14], were significantly or tended to be
145 higher in the organoids on day 5 than in those on day 1 (Supplementary Fig. 1G-1I). However,
146 the mRNA levels of a differentiated Paneth cell marker *Lyz1* did not differ between the
147 organoids on day 1 and day 5 (Supplementary Fig. 1J). These data suggest that intestinal
148 organoids on day 5 are richer in differentiated enterocytes, goblet cells, and enteroendocrine
149 cells, but not Paneth cells, than those on day 1. We analyzed miRNA expression profiles in the
150 intestinal crypt/villus fractions and organoids by microarray and detected 1,214 miRNAs
151 (Supplementary Table 2). Scatter plots comparing globally normalized signal intensities of
152 miRNAs showed that the miRNA expression levels were moderately correlated between the
153 crypt and villus fractions ($r$=0.64, Fig. 1A). The miRNA levels were highly correlated between
154 the organoids on day 1 and day 5 ($r$=0.96, Fig. 1B). Between the crypt/villus fractions and
155 organoids, the miRNA levels correlated highly, with Pearson's coefficient above 0.70 in all
156 cases (Fig. 1C-1F), indicating that organoids resemble intestinal epithelial cells in their miRNA
157 profiles. In particular, the highest correlation was observed between the organoids on day 5 and
158 the crypt fraction ($r$=0.91, Fig. 1D). However, it is noteworthy that there are some miRNAs,
159 including mmu-miR-143-3p and -145a-5p, in which the levels were extremely high in the villus
160 fraction but undetectable in the organoids on day 5 (Fig. 1F).
161
162 *Expression of some miRNAs are differentially regulated along the crypt-villus axis of*
163 *intestinal epithelium in mice.*
164 Although the levels of most miRNAs were similar between the crypt and villus fractions,
165 substantial numbers of miRNAs were expressed at different levels (Fig. 1A). Microarray
166 analysis showed that the levels of 56 miRNAs were higher in the villus fraction than in the crypt
167 fraction by more than four-fold (Fig. 2A). We performed qRT-PCR to compare 13 miRNAs in
168 which the levels were higher in the villus fraction than in the crypt fraction by more than
169 ten-fold. Seven miRNAs, mmu-miR-145a-5p, -143-3p, -199a-3p, -451a, 7027-5p, -125b-5p,
170 and 199a-5p, were significantly or somewhat higher in the villus than in the crypt fraction (Fig.

2C), whereas the other six miRNAs were not significantly different (Supplementary Fig. 2). Among the 12 miRNAs in which the levels were higher in the crypt than in the villus fraction by more than four-fold as shown by microarray (Fig. 2B), mmu-miR-3084-3p and -1839-39 were significantly or somewhat higher in the crypt than in the villus fraction (Fig. 2C). However, the other eight miRNAs were the same between the fractions (Supplementary Fig. 2).

*Expression of some mRNAs may be regulated by miRNAs along the crypt-villus axis of intestinal epithelium in mice.*

We predicted target genes of nine miRNAs in which the different expression levels between the crypt and villus fractions were validated by qRT-PCR. Among 103 genes that overlapped with the four prediction tools, we selected 15 manually according to GO biological process terms describing cell proliferation, cell differentiation, or cell death (Table 1). qRT-PCR analysis showed that the mRNA levels of six predicted target genes, *Cited2, Dach1, Pdcd4, Etv6, Lmo4,* and *Fzd6*, were significantly lower in the villus than in the crypt fraction (Fig. 3). Thus, these genes were expressed inversely from their corresponding miRNAs, suggesting that they may be regulated by their corresponding miRNAs. The mRNA levels of the other six genes, *Dusp6, Foxo1, Tbx1, Ywhaz, Sirt1,* and *Rnf144b*, were the same between the fractions, and the levels of *Rac1* were significantly higher in the villus than in the crypt fraction (Supplementary Fig. 3). The mRNA levels of *Ambn* and *Foxc2* were undetectable.

*Maturation process of murine intestinal organoids does not reflect the crypt-villus axis of intestinal epithelium in terms of miRNA profile.*

To compare the maturation process of intestinal organoids and intestinal epithelium along the crypt-villus axis in terms of miRNA profiles, we constructed a heat map of miRNAs in the crypt/villus fractions and the organoids on day 1 and day 5 (Fig. 4A). Only 25 miRNAs with different expression levels between the crypt and villus fractions as shown in Fig. 2A and 2B are listed. The heat map showed no clear differences in the levels of these miRNAs between the organoids on day 1 and day 5. We further examined some miRNAs and their target mRNAs by

qRT-PCR. The levels of mmu-miR-145a-5p, -143-3p, and -125b-5p were significantly lower in the organoids on day 5 than in those on day 1, and the mmu-miR-3084-3p levels were the same between the organoids (Fig. 4B). In addition, the mRNA levels of *Cited2, Dach1,* and *Pdcd4* were significantly higher in the organoids on day 5 than those on day 1 (Fig. 4C). Thus, maturation process of intestinal organoids does not reflect the crypt-villus axis of intestinal epithelium in terms of miRNA profile and their target genes.

## Discussion

To our knowledge, the present study is the first to compare miRNA expression profiles between isolated intestinal epithelial cells and cultured intestinal organoids. The data demonstrated that murine intestinal organoids largely resemble intestinal epithelium in their miRNA profiles. In addition, in order to examine whether maturation process of intestinal organoids reproduces the crypt-villus axis of intestinal epithelial cells in their miRNA expression profiles, the present study compared the miRNA profiles in the crypt and villus fractions and intestinal organoids cultured on day 1 and day 5. We observed that the miRNA expression profiles were most highly correlated between organoids on day 5 and the crypt fraction. Organoids on day 5 showed the typical characteristics of mature organoids in their morphology and the expression of marker genes for differentiated enterocytes, goblet cells, and enteroendocrine cells, suggesting that organoids on day 5 include differentiated cells, in their villus-like regions. Nevertheless, crypt-like regions comprise of the major portion of mature organoids. Together, mature organoids may provide a useful *in vitro* model to investigate miRNA expression in intestinal crypt epithelial cells.

Clearly, substantial numbers of miRNAs were differentially expressed between the crypt/villus fractions and organoids. It is particularly notable that some miRNAs, including mmu-miR-143-3p and -145a-5p with extremely high levels in the villus fraction, were undetectable in the organoids on day 5 (Fig. 1F). In the organoids on day 1, however, these two miRNAs were detected, although the expression levels were quite different from the villus fraction (Fig. 1E). From these results, we speculate that different expression levels of some

227 miRNAs between the crypt/villus fractions and organoids might reflect contamination by
228 non-epithelial cells in the crypt/villus fractions. Indeed, previous studies demonstrated that
229 miR-143/145 are expressed in mesenchymal cells and not epithelial cells in the intestine [15,
230 16]. It is possible that mmu-miR-143-3p and -145a-5p in the organoids on day 1 are derived
231 from surviving mesenchymal cell contamination.
232 Alternatively, the different expression levels of some miRNAs between the crypt/villus
233 fractions and organoids might reflect the absence of luminal factors including dietary
234 constituents and gut microbiota in the organoids. In addition, organoids also lack endocrine,
235 nervous, and immune systems. Therefore, it is likely that the expression of some miRNAs may
236 be regulated by such factors. In other words, organoids provide a useful *in vitro* model to test
237 whether these factors influence miRNA expression in intestinal epithelial cells.
238 We observed that some miRNAs were differentially expressed between crypt and villus
239 fractions, although the levels of most miRNAs were similar between them, being in line with
240 previous studies [8, 10]. These findings suggest that most miRNAs are not regulated during the
241 cell renewal process, i.e., cell proliferation, cell differentiation, and cell death, along the
242 crypt-villus axis in the intestine. However, the present study was substantially different from
243 those previous studies in the miRNA profiles. Although RNA samples in the present study were
244 isolated from epithelial cells in the villus and crypt fractions, McKenna *et al.* [8] isolated the
245 samples from intestinal mucosal scrapings. Therefore, miRNAs expressed in non-epithelial
246 cells would have been included in the analysis. Indeed, the miRNA profiles in McKenna *et al.*
247 [8] were different from those in Zhang *et al.* [10] in which the RNA samples were isolated from
248 epithelial cells. In addition, Zhang *et al.* [10] employed a miRNA PCR panel in which 750
249 miRNAs were probed and then detected 239 miRNAs per sample, while the present study
250 employed a miRNA microarray that contains 1,900 miRNA probes and then detected 1,214
251 miRNAs per sample. Thus, miRNA profile data would be profoundly influenced by sample
252 preparation and analytical method.
253 The present study showed that the number of miRNAs expressed specifically in the villus
254 fraction was much larger than the number of miRNAs expressed specifically in the crypt

fraction. Given that the different types of terminally differentiated cells has different miRNA profiles, it seems likely that the villus fraction consisting of three types of terminally differentiated cells (enterocytes, goblet cells, and enteroendocrine cells) has more diverse profiles of miRNAs as compared to the crypt fraction that consists mainly of immature transit-amplifying cells.

The miRNAs differentially expressed in the crypt and villus fractions in the present study have been reported to be associated with the pathophysiology of intestinal disorders. Ng *et al*. [17] reported that hsa-miR-451a is highly expressed in the intestinal tissue of infants with necrotizing enterocolitis as compared with normal tissue and is inversely correlated with the expression of Toll-like receptor 4 (TLR4), suggesting that hsa-miR-451 is involved in the pathogenesis of enterocolitis through TLR4 signaling defects. Zhou *et al.* [18] showed that the expression of hsa-miR-199a/b is decreased in the large intestinal tissue of patients with diarrhea-predominant irritable bowel syndrome (IBS-D) and is correlated with increased visceral pain. Martínez *et al.* [19] reported that hsa-miR-125b is involved in epithelial barrier function dysregulation in the small intestines of patients with IBS-D. In the present study, the levels of mmu-miR-451a, -199a-5p, and -125b-5p were significantly higher in the villus fraction than in the crypt fraction, suggesting that the expression of these miRNAs is regulated during the cell renewal process along the crypt-villus axis. Elucidating this regulatory mechanism may lead to the establishment of treatment strategies for the intestinal diseases.

The present study predicted *Cited2, Dach1*, and *Pdcd4* as target genes for mmu-miR-145a-5p. In addition, *Lmo4* and *Etv6* were predicted for mmu-miR-143-3p. The mRNA expressions of these genes were validated by qRT-PCR. De Gasperi *et al*. [20] demonstrated that *Cited2* is a target of miR-145 in skeletal muscle. *Cited2* is a transcriptional regulator that modulates signaling through NF-κB, Smad3, and other transcription factors. However, the authors showed unchanged protein levels of *Cited2* in muscle with decreased miR-145. Sum *et al.* [21] showed by immunohistochemistry that *Lmo4* protein is abundantly expressed in the epithelial cells of small intestinal crypts in mice. The authors mentioned that *Lmo4* plays an important role in the regulation of epithelial cell proliferation and in cancer

pathogenesis. The present study showed that mmu-miR-143-3p was highly expressed in the villus fraction and that the mRNA levels of its predicted target *Lmo4* were lower in the villus fraction. Considering that miR-143 is expressed in mesenchymal cells but not epithelial cells in the intestine [15, 16], it is likely that, around the intestinal villi, miR-143-3p expressed in mesenchymal cells suppresses the expression of *Lmo4*, which may contribute to the termination of epithelial cell proliferation. Further studies are needed to clarify such interactions between mesenchymal and epithelial cells through miRNA-mediated regulation in the intestine. Additionally, the present study predicted *Fzd6* as a target for mmu-miR-199a-5p. The results are in line with a previous study showing that *FZD6* is highly expressed in the tumor tissues of patients with colorectal cancer and is negatively regulated by miR-199a-5p in colorectal cancer cells [22]. *Fzd6* is a kind of Wnt receptor that regulates cell proliferation, cell differentiation, and cell death. Thus, highly expressed mmu-miR-199a-5p may be involved in the repression of cell proliferation and the promotion of cell differentiation via suppression of *Fzd6* expression in villus epithelium. Together, the present findings suggest that some miRNAs, including mmu-miR-143-3p and -199a-5p, are involved in the regulation of epithelial cell renewal via control of target genes along the crypt-villus axis of the intestine.

Nevertheless, the differential expression of miRNAs and their target genes observed in the crypt and villus fractions were not reproduced during the maturation of intestinal organoids. This might be due to the lack of luminal factors and endocrine, nervous, and immune systems in the organoids as described above. In addition, different cell populations between *in vivo* samples and organoids might exist. Epithelial cells are much more abundant in villi as compared to crypts *in vivo*, whereas crypt regions are predominant in mature organoids.

In conclusion, the present study showed that murine intestinal organoids largely resemble intestinal epithelium in their miRNA profiles. However, the miRNA profile during the maturation process of organoids did not reflect the profile along the crypt-villus axis. Nevertheless, we propose that intestinal organoids provide a useful *in vitro* model to investigate miRNA expression in intestinal epithelial cells.

## Author contributions

K. S. developed the concept and designed the research. F. O. performed the experiments and analyzed the data. K.S. and F.O. prepared the manuscript. All authors read and approved the final version of manuscript.


## Funding

This work was supported in part by the Ministry of Education, Culture, Sports, Science and Technology Japan (MEXT) under the Grant-in-Aid for Scientific Research (no. 26292062); the MEXT under the Regional Innovation Strategy Support Program; and the MEXT and Japan Science and Technology Agency under the Center of Innovation Program.


## Disclosure statement

All authors have no conflict of interest to declare.

## References


[1] van der Flier LG, Clevers H. Stem cells, self-renewal, and differentiation in the intestinal epithelium. Annu Rev Physiol. 2009;71:241-260.

[2] Sato T, Stange DE, Ferrante M, et al. Long-term expansion of epithelial organoids from human colon, adenoma, adenocarcinoma, and Barrett's epithelium. Gastroenterology. 2011;141:1762-1772.

[3] Sato T, Vries RG, Snippert HJ, et al. Single Lgr5 stem cells build crypt-villus structures in vitro without a mesenchymal niche. Nature. 2009;459:262-265.

[4] Miyoshi H, Stappenbeck TS. *In vitro* expansion and genetic modification of gastrointestinal stem cells in spheroid culture. Nat Protoc. 2013;8:2471-2482.

[5] Ambros V. The functions of animal microRNAs. Nature. 2004;431:350-355.

[6] Bartel DP. MicroRNAs: genomics, biogenesis, mechanism, and function. Cell. 2004;116:281-297.

[7] Miska EA. How microRNAs control cell division, differentiation and death. Curr Opin

Genet Dev. 2005;15:563-568.

[8] McKenna LB, Schug J, Vourekas A, et al. MicroRNAs control intestinal epithelial differentiation, architecture, and barrier function. Gastroenterology. 2010;139:1654-1664

[9] Dalmasso G, Nguyen HT, Yan Y, et al. MicroRNAs determine human intestinal epithelial cell fate. Differentiation. 2010;80:147-154.

[10] Zhang Y, Viennois E, Zhang M, et al. PepT1 expression helps maintain intestinal homeostasis by mediating the differential expression of miRNAs along the crypt-villus axis. Sci Rep. 2016;6:27119.

[11] Tsuruta T, Saito S, Osaki Y, et al. Organoids as an *ex vivo* model for studying the serotonin system in the murine small intestine and colon epithelium. Biochem Biophys Res Commun. 2016;474:161-167.

[12] Edgar R, Domrachev M, Lash AE. Gene Expression Omnibus: NCBI gene expression and hybridization array data repository. Nucleic Acids Res. 2002;30:207-210.

[13] Haegebarth A, Bie W, Yang R, et al. Protein tyrosine kinase 6 negatively regulates growth and promotes enterocyte differentiation in the small intestine. Mol Cell Biol. 2006;26:4949-4957.

[14] Brodrick B, Vidrich A, Porter E, et al. Fibroblast growth factor receptor-3 (FGFR-3) regulates expression of paneth cell lineage-specific genes in intestinal epithelial cells through both TCF4/beta-catenin-dependent and -independent signaling pathways. J Biol Chem. 2011;286:18515-18525.

[15] Chivukula RR, Shi G, Acharya A, et al. An essential mesenchymal function for miR-143/145 in intestinal epithelial regeneration. Cell. 2014;157:1104-1116.

[16] Kent OA, McCall MN, Cornish TC, et al. Lessons from miR-143/145: the importance of cell-type localization of miRNAs. Nucleic Acids Res. 2014;42:7528-7538.

[17] Ng PC, Chan KY, Leung KT, et al. Comparative miRNA expressional profiles and molecular networks in human small bowel tissues of necrotizing enterocolitis and spontaneous intestinal perforation. PLoS One. 2015;10:e0135737.

[18] Zhou Q, Yang L, Larson S, et al. Decreased miR-199 augments visceral pain in patients

with IBS through translational upregulation of TRPV1. Gut. 2016;65:797-805.

[19] Martínez C, Rodiño-Janeiro BK, Lobo B, et al. miR-16 and miR-125b are involved in barrier function dysregulation through the modulation of claudin-2 and cingulin expression in the jejunum in IBS with diarrhoea. Gut. 2017;66:1537-1538.

[20] De Gasperi R, Graham ZA, Harlow LM, et al. The signature of microRNA dysregulation in muscle paralyzed by spinal cord injury includes downregulation of microRNAs that target myostatin signaling. PLoS One. 2016;11:e0166189.

[21] Sum EY, O'Reilly LA, Jonas N, et al. The LIM domain protein Lmo4 is highly expressed in proliferating mouse epithelial tissues. J Histochem Cytochem. 2005;53:475-486.

[22] Kim BK, Yoo HI, Kim I, et al. FZD6 expression is negatively regulated by miR-199a-5p in human colorectal cancer. BMB Rep. 2015;48:360-366.

325

**Table 1.** miRNAs differentially expressed between crypt and villus fractions isolated from murine small intestine and their predicted target genes

| miRNA | Target gene | | | | |
|---|---|---|---|---|---|
| mmu-miR-145a-5p | *Cited2* | *Dach1* | *Dusp6* | *Foxo1* | *Pdcd4* |
| mmu-miR-143-3p | *Etv6* | *Lmo4* | | | |
| mmu-miR-199a-3p | - | | | | |
| mmu-miR-451a | *Rac1* | *Tbx1* | *Ywhaz* | | |
| mmu-miR-7027-5p | - | | | | |
| mmu-miR-125b-5p | - | | | | |
| mmu-miR-199a-5p | *Fzd6* | *Sirt1* | | | |
| mmu-miR-3084-3p | *Rnf144b* | | | | |
| mmu-miR-1839-3p | *Ambn* | *Foxc2* | | | |

Only nine miRNAs validated by qRT-PCR as shown in Fig. 2C are listed.

340 **Figure Caption**

341 **Figure 1** Scatter plots of intestinal miRNA expression detected using microarray analysis to
342 compare between crypt and villus fractions (*A*), organoids on day 1 and day 5 (*B*), crypt fraction
343 and organoids on day 1 (*C*), crypt fraction and organoids on day 5 (*D*), villus fraction and
344 organoids on day 1 (*E*), and villus fraction and organoids on day 5 (*F*). The expression level of
345 each miRNA was globally normalized such that the median of all miRNAs for each sample was
346 25. Dotted lines indicate the boundaries of miRNAs expressed at four-fold higher and lower
347 levels. Pearson's correlation coefficient (*r*) in each plot is shown. Plots depicted in red show
348 miRNAs differentially expressed in crypt and villus fractions and validated by qRT-PCR as
349 shown in Fig. 2C.
350

351 **Figure 2** Relative expression levels of miRNAs in crypt and villus fractions isolated from
352 murine small intestine. *A,* Ratio of villus to crypt fractions of miRNAs detected using
353 microarray analysis. Fifty-six miRNAs in which the ratio was more than four-fold are plotted.
354 Abbreviated names of each miRNA in which the ratio was more than ten-fold are shown. *B,*
355 Ratio of crypt to villus fractions of miRNAs detected using microarray analysis. Twelve
356 miRNAs in which the ratio was more than four-fold are plotted, and abbreviated names of each
357 miRNA are shown. *C*, Comparison of miRNA expression levels between crypt and villus
358 fractions isolated from murine small intestine. The miRNA levels in each sample (n=6 in each
359 fraction) were estimated by qRT-PCR. In each graph, values with asterisks are significantly
360 different *vs.* crypt fraction ($P<0.05$).
361

362 **Figure 3** Relative mRNA levels of predicted target genes of miRNAs in crypt and villus
363 fractions isolated from murine small intestine. The miRNA levels in each sample (n=6 in each
364 fraction) were estimated by qRT-PCR. In each graph, values with asterisks are significantly
365 different *vs.* crypt fraction ($P<0.05$).
366

**Figure 4** *A*, Heat map of miRNA expression levels determined using microarray analysis to compare crypt and villus fractions isolated from murine small intestine and murine intestinal organoids on day 1 and day 5. Only 25 miRNAs with different expression levels between crypt and villus fractions as shown in Fig. 2A and 2B are listed. Red and green indicate higher and lower levels, respectively. *B*, Relative expression levels of miRNAs in murine intestinal organoids on day 1 and day 5. *C*, Relative mRNA levels of predicted target genes of miRNAs in organoids on day 1 and day 5. The miRNA and mRNA levels were estimated in each sample (n=3 on day 1 and day 5) by qRT-PCR. In charts *B* and *C*, values with asterisks are significantly different *vs.* organoids on day 1 ($P<0.05$).

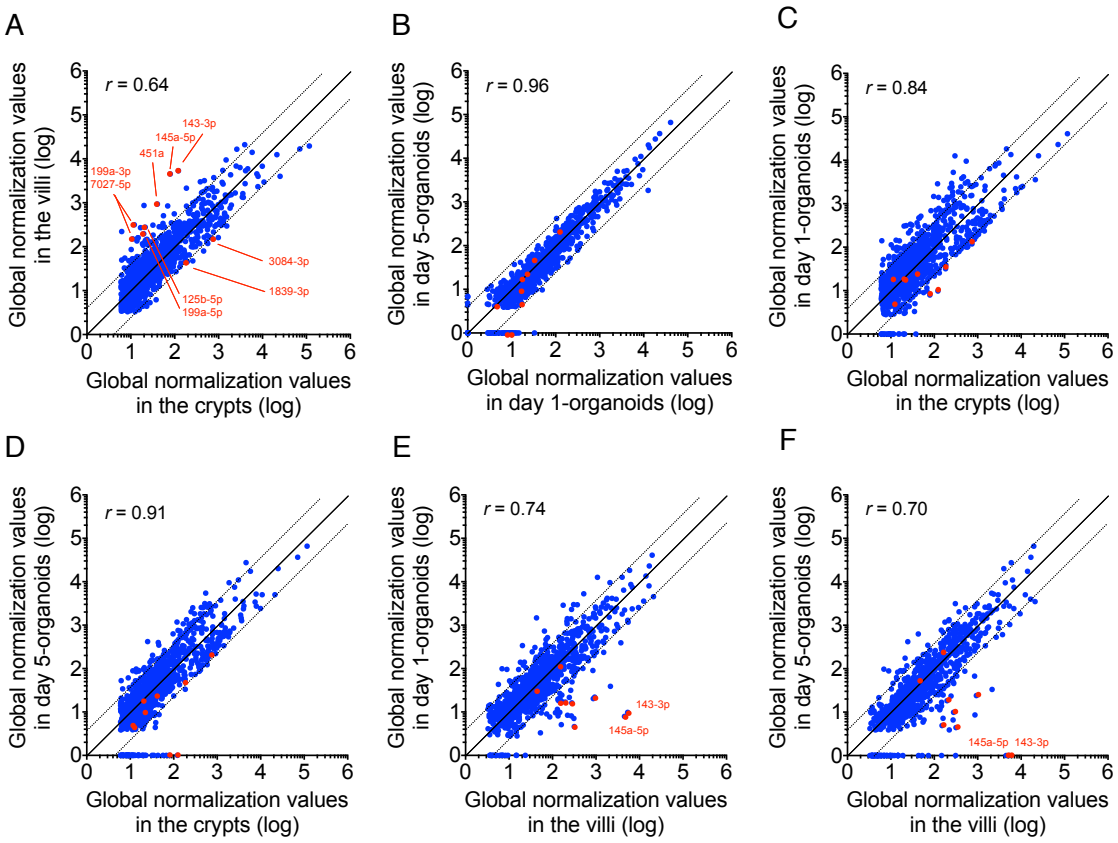


Fig. 1 Ohsaka and Sonoyama

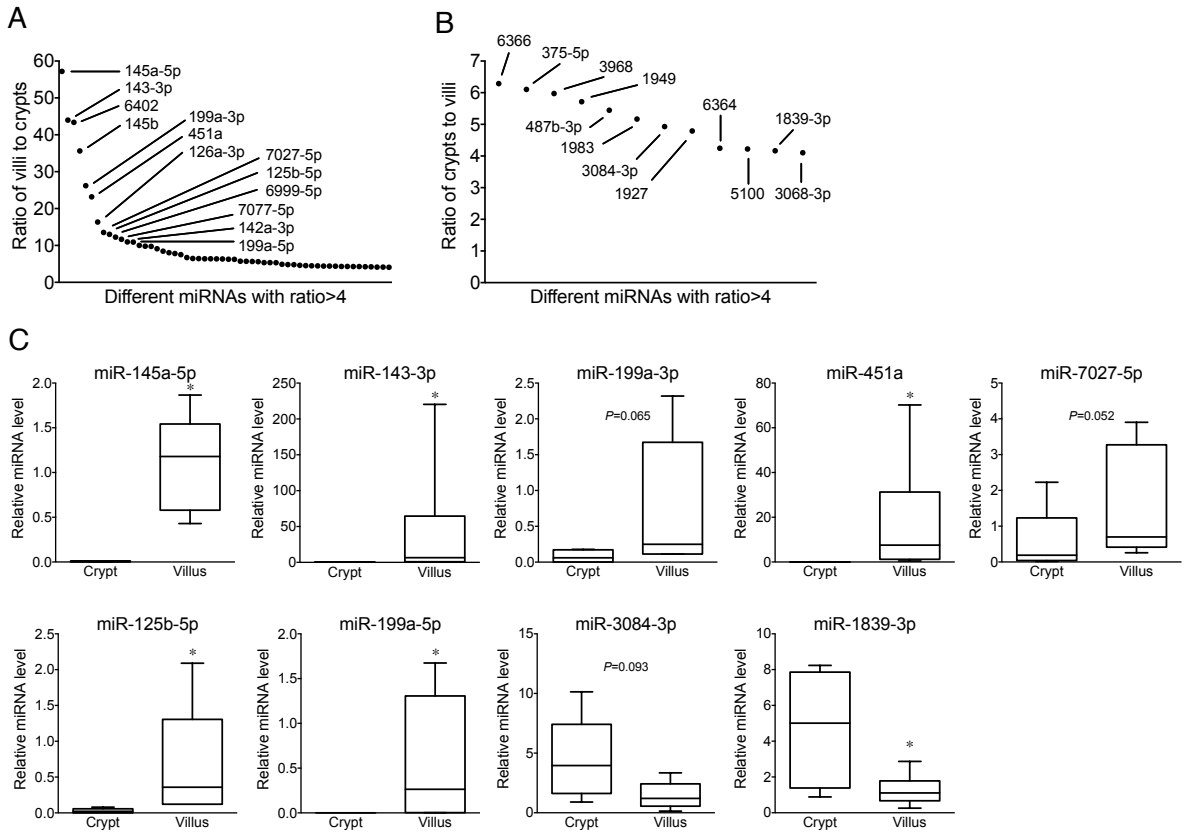


Fig. 2 Ohsaka and Sonoyama

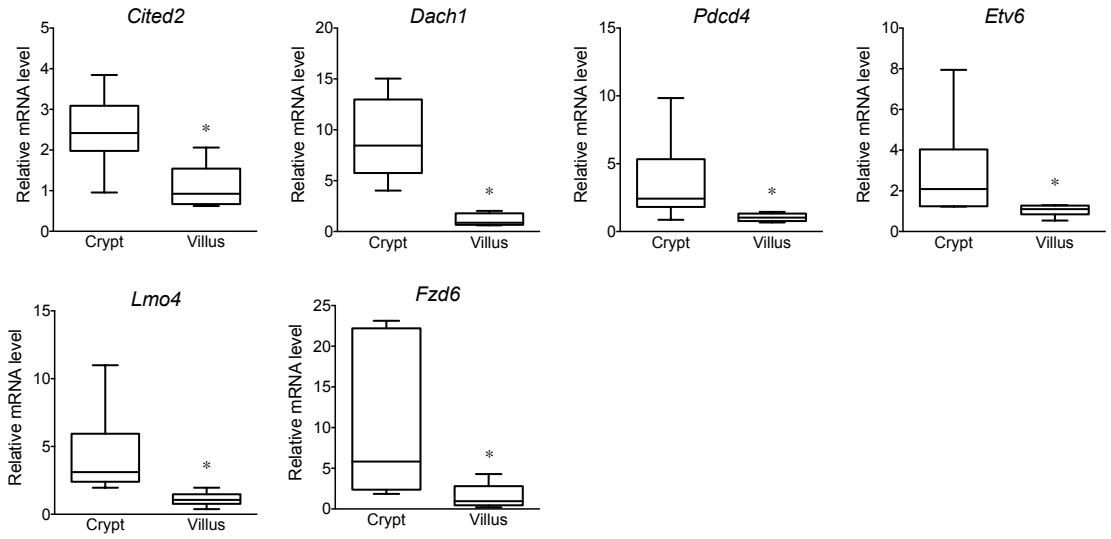


Fig. 3 Ohsaka and Sonoyama

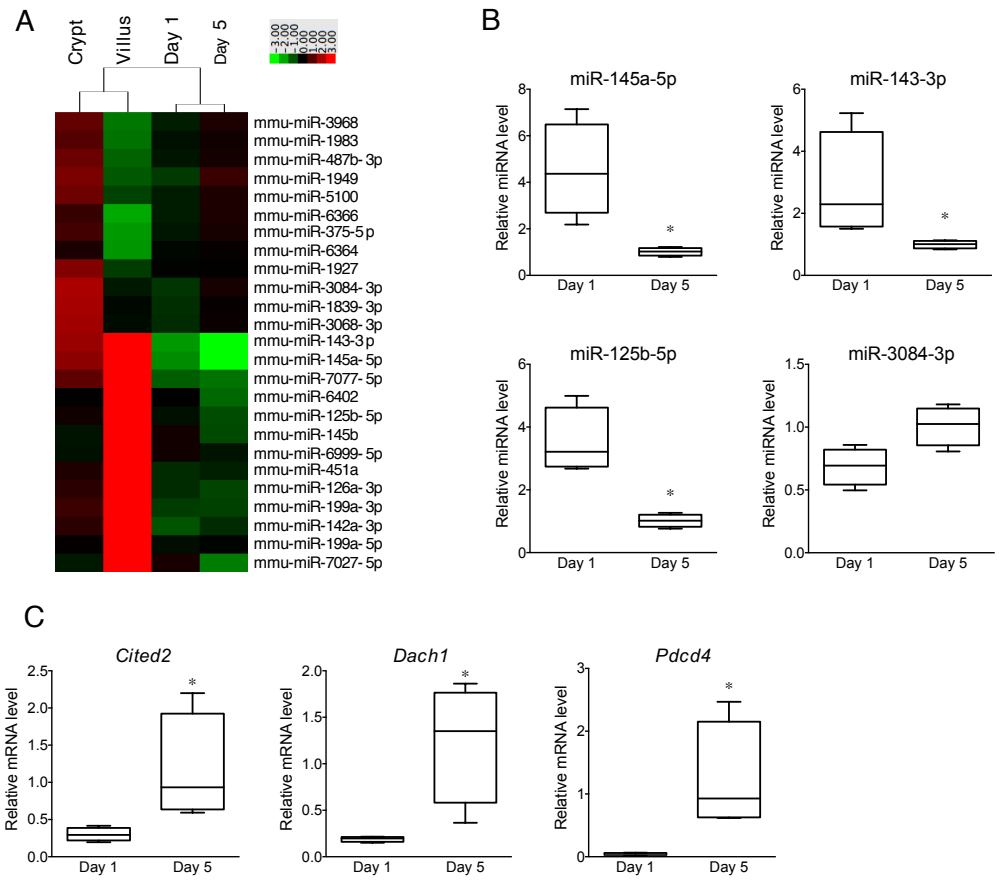


Fig. 4 Ohsaka and Sonoyama

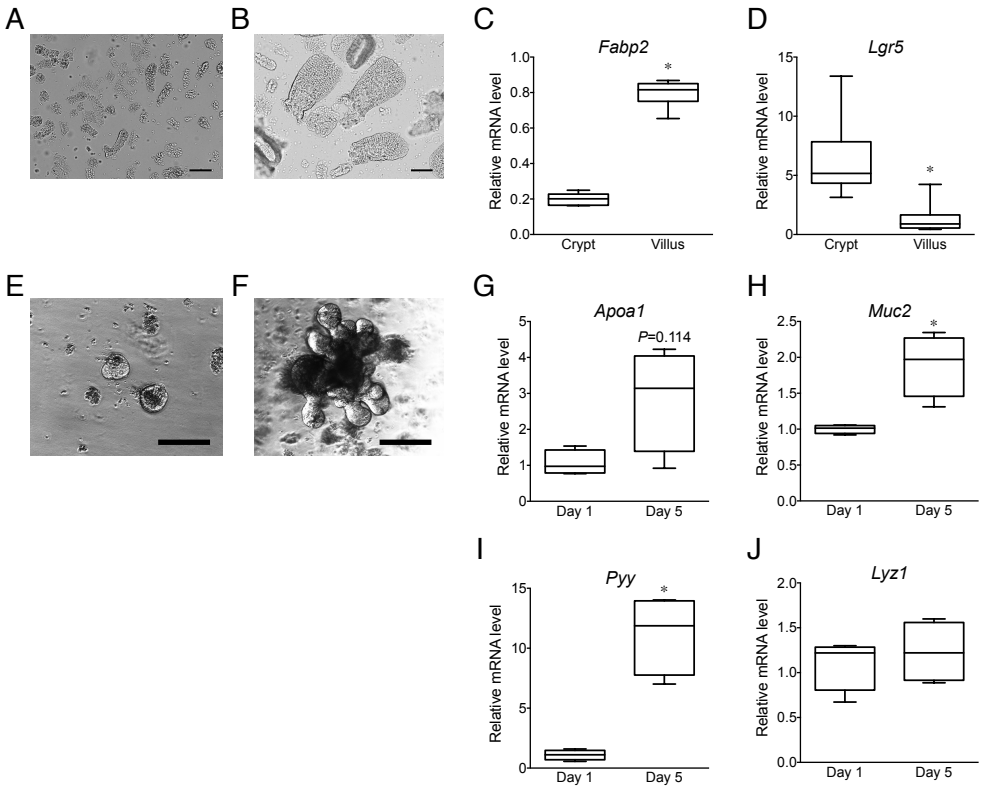


Supplementary Fig. 1 Charts A and B show light-microscopic visualizations of crypt and villus fractions, respectively, isolated from murine small intestine. Charts C and D show comparisons of mRNA levels of *Fabp2* and *Lgr5* between crypt and villus fractions. Charts E and F show light-microscopic visualizations of intestinal organoids on day 1 and day 5, respectively. Charts G-J show comparisons of mRNA levels of *Apoa1, Muc2, Pyy,* and *Lyz1*, differentiation markers of enterocytes, goblet cells, enteroendocrine cells, and Paneth cells, respectively, between organoids on day 1 and day 5. Scale bars indicate 100 $\mu$m in charts A and B and 200 $\mu$m in charts E and F. In charts C,D, and G-J, mRNA levels were estimated in each sample (n=6 in crypt and villus fractions and n=3 in organoids on day 1 and day 5) by qRT-PCR, and values with asterisks are significantly different ($P$<0.05).

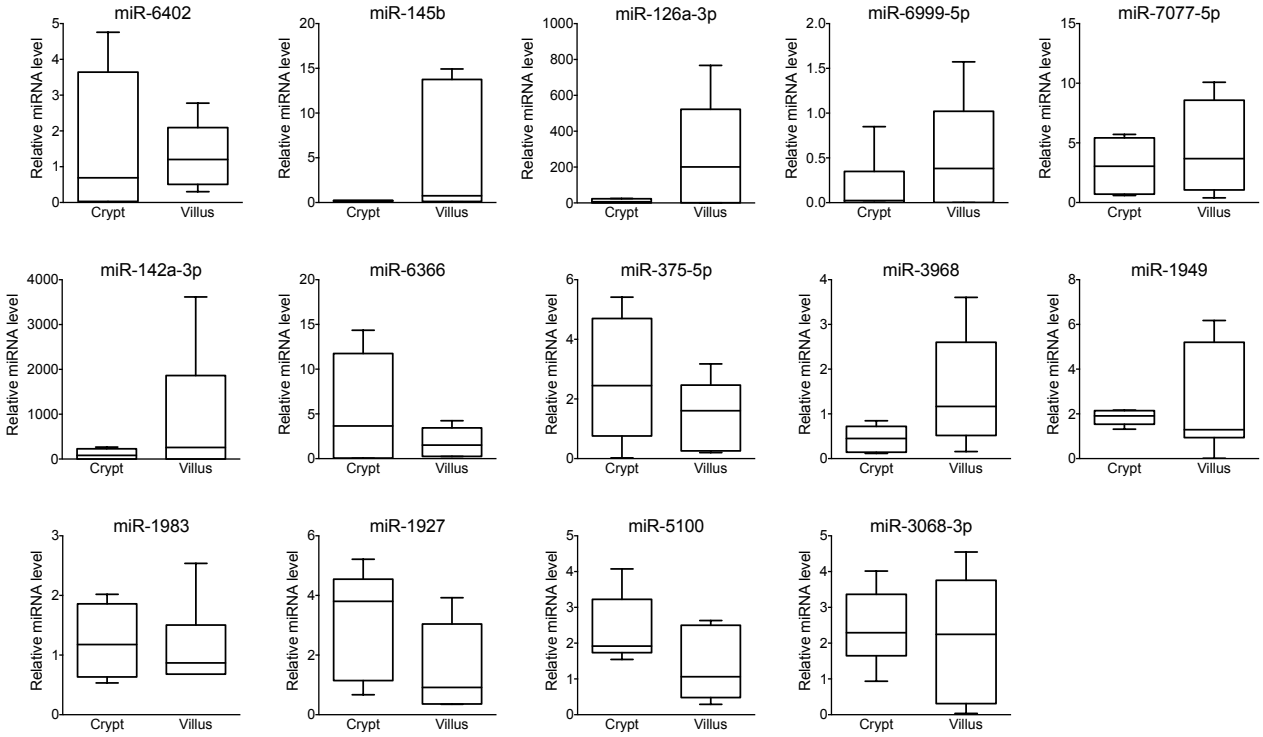


Supplementary Fig. 2 Comparison of miRNA expression levels between crypt and villus fractions isolated from murine small intestine. The miRNA levels in each sample (n=6 in each fraction) were estimated by qRT-PCR.

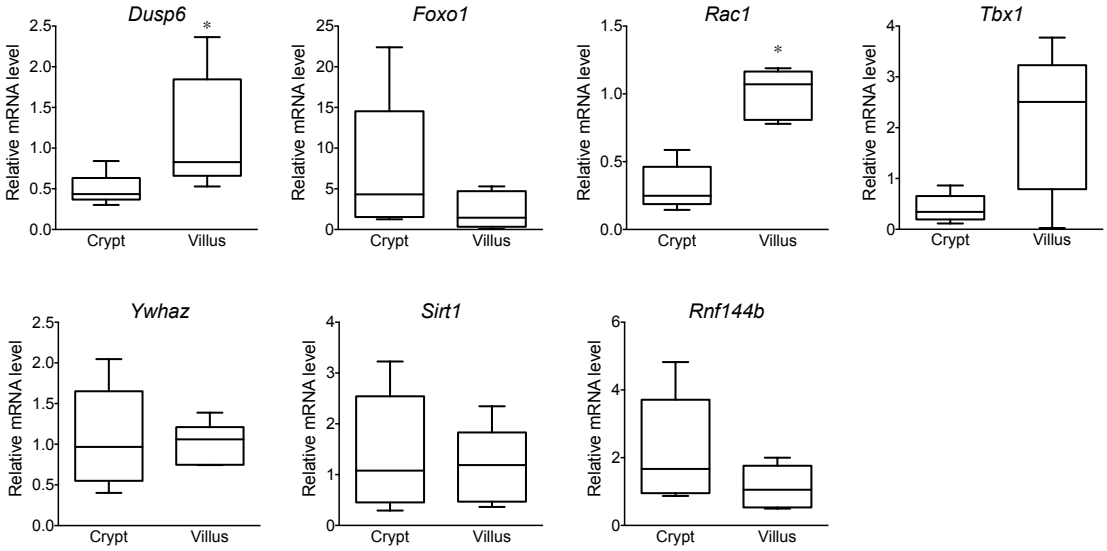


Supplementary Fig. 3 Comparison of mRNA expression levels between crypt and villus fractions isolated from murine small intestine. The mRNA levels in each sample (n=6 in each fraction) were estimated by qRT-PCR. In each graph, values with asterisks are significantly different vs. crypt fraction ($P$<0.05).